A Calorimetric Investigation of the Copper-Zinc System

KRISHNA PARAMESWARAN AND GEORGE HEALY

A high temperature, high-speed adiabatic calorimeter was used to measure the heat content of alloys in the copper-zinc system. These measurements were then used, along with the results of other investigators, in calculating thermodynamic properties of copper-zinc alloys. These included: heats of formation of liquid copper-zinc alloys, of alpha, beta, gamma, and epsilon phases at different temperatures, and of delta phase at 900 K (which was not available in literature), and excess entropies of formation for the alpha, beta prime, gamma, epsilon phases and the heat effect for the beta-beta prime transformation.

INTRODUCTION

THERMODYNAMIC properties of copper-zinc alloys have been obtained from activity measurements and calorimetric determinations. Lumsden[1] reviewed much of the early work on the thermodynamics of the copper-zinc system. A more recent review was presented by Hultgren *et al.*[2] The high vapor pressure of zinc at elevated temperatures has been a major source of experimental difficulties.

A. Activity Measurements

The most common activity measurement technique utilized has been determination of the vapor pressure of zinc over copper-zinc alloys of known composition. Hargreaves[3] used a differentially heated quartz tube and measured the condensation temperature of the heated brass at the other end of the tube. Herbenar *et al*[4] determined the vapor pressure of zinc over various alloys at a number of temperatures from atomic spectra data. Kubaschewski and Caterall[5] calculated the integral heats of formation of solid copper-zinc alloys from solid metals. Pemsler and Rapperport[6,7] used atomic absorption, with a hollow cathode lamp as the radiation source, to determine the activity of zinc in solid copper-zinc alloys. This technique is an improvement over the spectrophotometric method for measuring small vapor pressures in static absorption cells.

Argent and Wakeman[8] calculated thermodynamic properties for zinc in copper from vapor pressure measurements using the dew point method. Olander[9] used emf measurements to determine the activity of zinc at temperatures ranging from 685 to 899 K for copper-zinc alloys containing 44 to 84 at. pct zinc. Kleppa and Thalmayer[10] also used emf measurements to determine activities in liquid alloys at 900 K for alloys containing 80 to 92 at. pct zinc. Downie[11] measured the vapor pressure of zinc by the dew point determination of liquid alloys containing 25 to 68 at. pct zinc at 1200 K. Everett, Jacobs, and Kitchner[12] used a transportation method to determine the activities in liquid alloys. Baker[13] measured the boiling point of liquid copper-zinc alloys, at various pressures in the temperature range of 1373 to 1473 K.

B. Calorimetry

Of the many types of calorimeters, "drop" calorimeters have been commonly used in the study of high temperature thermal properties. In this type of calorimetry, the sample is heated to a known temperature and then dropped into the calorimeter heat sink—usually operated around room temperature. Various types of heat sinks have been devised and include fluids such as: water, aniline and paraffin oil, a metal vessel submerged in water, mixtures such as ice, water, and frozen and liquid ether, and a massive block of metal, such as copper or aluminum, surrounded by a constant temperature bath, or by an adiabatic shield. Apart from many experimental difficulties, relatively accurate data can be obtained by proper design of the furnace, dropping mechanism, heat sink, and measuring system. One of the main disadvantages of this type of calorimeter in terms of time and labor, however, is that only the total heat content of the sample from the equilibrium temperature, usually room temperature to a certain elevated temperature, can be obtained in a single run. Therefore, several runs have to be made to measure the heat content over a range of temperatures and to determine the heat of transformation. This disadvantage may be eliminated by several other calorimeters which employ adiabatic heating or cooling methods to obtain specific heats and/or heats of transformation. Oelsen's[14-16] method of continuous quantitative thermal analysis was selected, as it permits a complete enthalpy-temperature diagram to be obtained from the results of a single experiment.

APPARATUS

The major parts of the apparatus, which stands about 3 m high, are shown in Fig. 1. It is comprised of:

a furnace for heating the sample,
a heat sink for measuring the heat it releases,
a thermocouple to measure its temperature during this time,
a mechanism for moving the sample and thermo-

KRISHNA PARAMESWARAN is on the Professional Staff of Arthur D. Little, Inc., Cambridge, MA 02140 and GEORGE W. HEALY, formerly with the Department of Metallurgy at Pennsylvania State University, is now with the Department of Mining, Metallurgy and Fuels at the University of Utah, Salt Lake City, UT 84112.

Manuscript submitted May 22, 1978.

ISSN 0360-2141/78/1211-0657$00.75/0

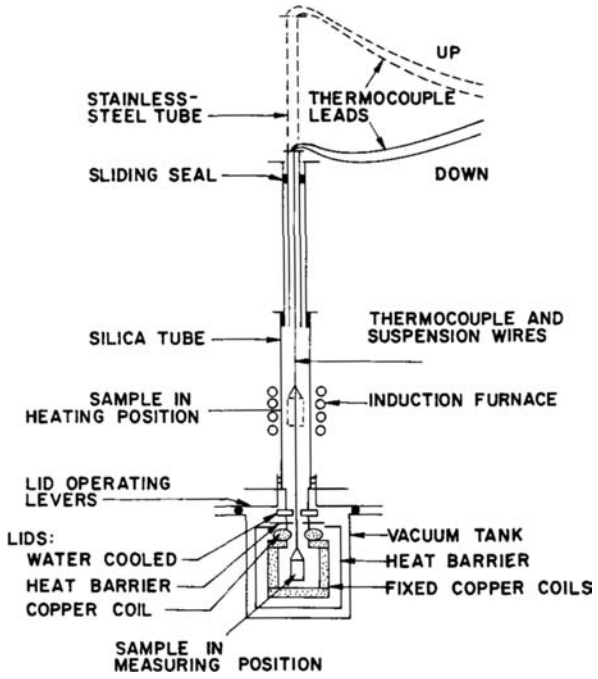

Fig. 1—The calorimeter assembly.

couple rapidly from the furnace to the heat sink, and an adiabatic shield and enclosure that surrounds the whole apparatus, so that an inert atmosphere or vacuum can be maintained.

The heat sink is based on the principle described by Yamaguchi.[17,18] The heat sink is composed of three fixed and two movable coils. Each is wound with 1.63 mm diam enamelled copper wire fixed in place by epoxy, and weighs about 25 Kg. The coils enclose a cavity 180 mm in diam by 200 mm high and are connected in series.

The coil assembly is surrounded by an adiabatic shield wound with 0.9 mm chromel heating wire. A 10 junction array of differential thermocouples is cemented to the shield and to the outside of the coil at alternate junctions. This differential thermocouple array is used to signal a current adjusting type (CAT) controller. This device controls the current to the chromel heating wire based on the temperature difference between the adiabatic shield and the outside of the calorimeter coil.

The samples are contained in a silica crucible (96 pct SiO_2). The crucible is suspended from a sliding stainless-steel tube (Fig. 1, top), using a molybdenum wire harness. A thermocouple made of 0.46 mm chromel-alumel wire travels up or down with the crucible and sample. When the crucible and charge are at their upper position, they are centered in a section of a silica tube that is surrounded by an induction furnace. In its lower position, they are centered inside the copper coil assembly.

Figure 2 shows the sample and its thermocouple in the calorimeter coil. The heat sink coil windings are connected to the resistance measuring circuit, a wheatstone bridge, the imbalance of which is recorded by the Y-function of the high-speed X-Y recorder. The thermocouple output goes to the X-function of the recorder. The potentiometer serves to change the range on the X-function of the recorder.

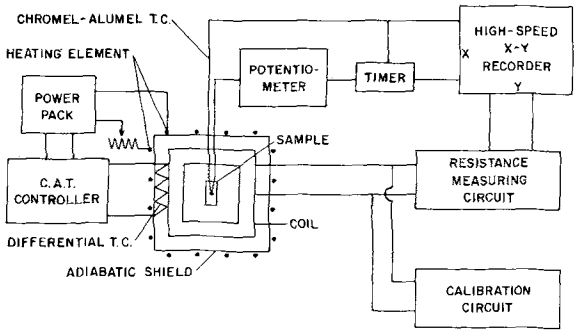

Fig. 2—Block diagram of measuring system.

Time signals are sent to the recorder every 30 s during experiments by short circuiting the thermocouple with an electrical timer.

Details of the measuring and standardizing circuits are shown in Fig. 3. The resistance-measuring circuit is to the left of S2-S3. (All resistances are secondary standards and the values are shown in ohms.) The potential across the bridge is obtained by measuring P3(t), using the known values of resistances R4 and R8. One side of the bridge is formed by resistances R2 and R3; the other by R1 and the parallel circuit comprised of resistance box RB and the coil resistance R(t). The variable resistor DR2 may be inserted in place of the coil during the time the sample is being heated. The purpose of the resistance box RB is to change the range of the Y-function of the recorder when necessary. WB represents a guarded wheatstone bridge.

EXPERIMENTAL PROCEDURE

The samples are prepared from weighed amounts of oxygen free, high-conductivity copper and 99.99 pct zinc. Both are in the form of 25 mm diam bar stock, which is drilled to receive a thermocouple. The sample is held in a silica crucible (96 pct SiO_2). The crucible is covered by an alumina cement lid, cast around a 6 mm diam silica tube. The latter serves to position thermocouple in the center of the melt. A typical charge weighs about 230 gm, while the crucible, thermocouple tube, and lid weigh about 40 gm.

The crucible with its charge and the thermocouple are suspended from the sliding stainless-steel tube before being raised to the heating position shown in Fig. 1. The assembly is then evacuated and backfilled with purified argon several times to ensure a low oxygen atmosphere. A small positive pressure of argon is maintained while the sample is heated in the induction furnace. During the heating period, the calorimeter coil and adiabatic enclosure are brought to equilibrium. When the sample temperature is about

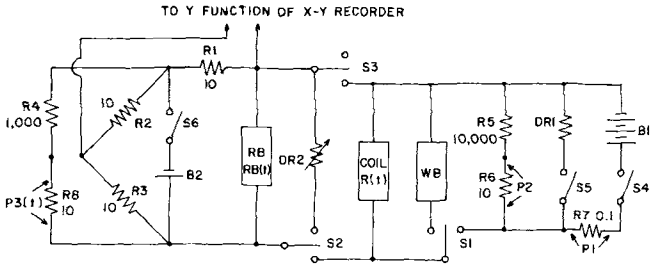

Fig. 3—Resistance-measuring and calibration circuits.

100 K above the liquidus temperature, it is held at temperature for 5 to 10 min. Longer times or higher superheat are avoided to minimize the loss of zinc by evaporation. The power to the furnace is then turned off, the X-Y recorder is activated, the calorimeter lids are opened, the sample is lowered into the calorimeter heat sink, the lids are closed, and the measuring part of the run is underway. This starting operation takes about 5 s.

Figure 4 shows a typical X-Y recorder trace. The X-axis shows the thermocouple output, while the Y-axis gives the imbalance of the wheatstone bridge circuit, indicating the increase in coil resistance as it warms up on receiving heat from the sample. The sample begins to freeze about 12 s after the run begins and is completely frozen at about 1 min and 20 s. A short time later it is necessary to adjust RB so that the pen does not go offscale. P3, the bridge voltage, is measured several times during the run. The remainder of the run represents cooling of the alloy in the solid state. The entire run lasted about 2 h.

Samples of the alloys used in the calorimeter runs were chemically analyzed by an atomic absorption technique on a Perkin-Elmer Model 305A unit. There were zinc losses due to volatilization. As most of the loss occurs during the heating and melting of the samples, the alloy composition was assumed to be that determined by the chemical analysis. The samples for X-ray phase identification were examined using a Norelco X-ray diffraction unit with Cu K_α radiation and a scanning rate of 2 deg (2θ) per min.

Calibration

The relation between the heat absorbed by the coil and its resistance change was determined by electrical calibration, yielding the following expression:

$$H_2 - H_1 = (R_2 - R_1)\,[42{,}030 + 717.5\,(R_2 + R_1) \pm 270]\ \text{cals}^*. \qquad [1]$$

*Factor for conversion to SI units are presented in Appendix I.

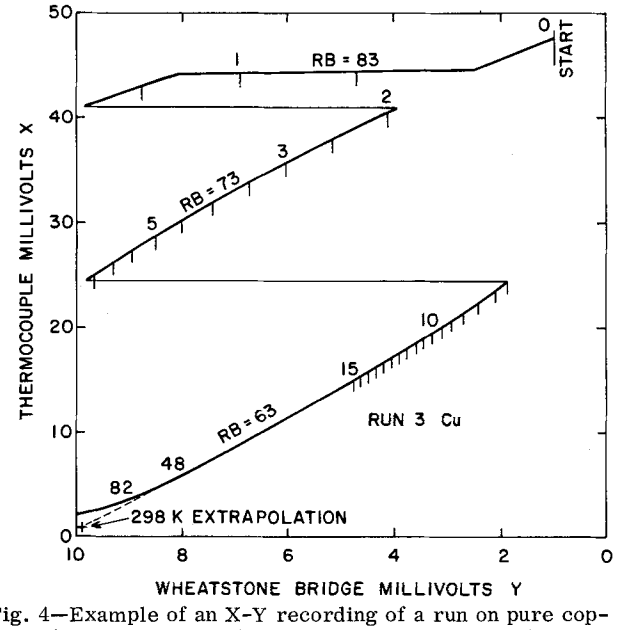

Fig. 4—Example of an X-Y recording of a run on pure copper. Short vertical marks indicate 30 s intervals while numbers above the curves indicate the elapsed time in minutes.

The relationship was the same whether electrical energy was introduced uniformly in the entire coil, or only in the inner half of the winding. This confirmed that the calibration was independent of temperature distribution.

Evaluation of Data

Data points were picked off the X-Y chart (Fig. 4) at suitable intervals on the temperature axis. For each point, the temperature of the sample was obtained from the thermocouple calibration. The coil resistance was calculated from the bridge imbalance Y and the circuit constants, including the bridge voltage P3 and the RB setting (Fig. 3). The total heat absorbed by the coil during a temperature interval was computed from the coil calibration. This gave the amount of heat that left the metal or alloy sample, silica crucible, alumina lid, and molybdenum wire harness in that interval. From the known weights of silica, alumina, and molybdenum wire an equivalent weight of silica (equal to SiO_2 + 1.07 Al_2O_3 + 0.28 Mo) was calculated. Kelly's enthalpy data[19] were then used to determine the heat liberated by the crucible, lid, and harness during the interval. Subtracting this heat release from the total heat absorbed by the coil yields the heat released by the metal or alloy sample.

Corrections

An empirical correction factor was derived to reflect the temperature difference between the container (silica crucible, alumina lid) and the metal sample, the nonuniformity of temperature in the container, the heat loss by conduction through the thermocouple, and any lack of adiabaticity of the shield.

The correction factor was estimated from runs with pure copper and pure zinc. The correction factor was computed as the difference between the experimentally determined value of heat content (computations as described in evaluation of data) and that selected by Hultgren *et al*[2] at each temperature. The correction factor in calories per run is plotted (Fig. 5) as a function of temperature. The curves at the extreme represent the correction factor derived from zinc and copper runs. Typically runs were made with 3.5 gm-atoms of the alloy. The maximum correction factor for the temperature range covered in the experiments was about 1300 calories per run or 370 cal/gm-atom.

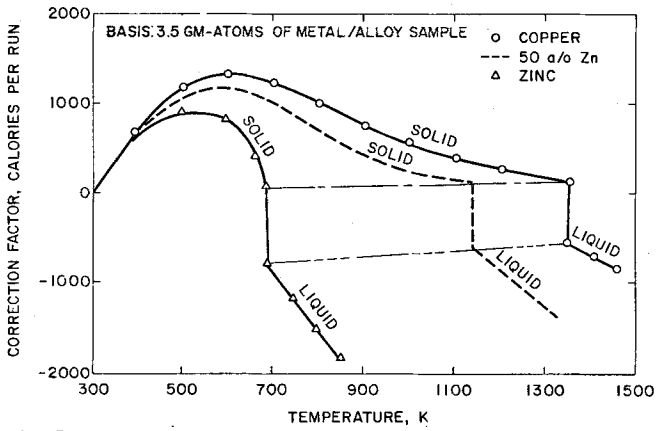

Fig. 5—Empirical correction factor.

Table I. Heats of Solidification of Copper and Zinc

Metal	Run	Melting Point, K	Heats of Solidification, cal/gm-atom	
			This Work	Hultgren *et al.*[2,20]
Copper	3	1356	3220	3120 ± 200
	10	1356	3250	
	21	1356	3270	
Zinc	11	692	1740	1750 ± 25
	16	692	1780	

As the weights of silica crucible, alumina lid, molybdenum harness wire, and sample (pure metal or alloy) did not vary significantly, the correction factor for alloys was assumed to be between that of pure copper and zinc. Consequently, for an alloy, an interpolated correction factor curve (interpolation guided by solidus and liquidus temperatures) was used. Such a curve, for a 50 at. pct zinc alloy, is shown as the dashed curve in Fig. 5. This correction factor was applied to correct the measured heat contents of alloys.

Estimate of Error Limits

In all, three runs were made with pure copper and two with pure zinc. The correction factor was applied to correct the measured heat contents for the copper and zinc runs. The scatter in the heat content data was evaluated statistically. For the heat-content measurement, the 95 pct confidence interval was ±180 cal/gm-atom, based on the dispersion of data and sample size using Student's t distribution.

EXPERIMENTAL RESULTS

Table I presents the heats of solidification and the melting points for copper and zinc obtained from the runs used to determine the correction factor. There is reasonable agreement for the heats of solidification with the selected values of Hultgren *et al.*[2,20] The melting points of copper and zinc agree well with generally accepted values.

The data, as examplified in Fig. 4, are evaluated to obtain a series of enthalpy temperature plots (shown in Figs. 6 to 10) for copper-zinc alloys containing 4.5 to 94.6 at. pct zinc. There is a discontinuity in these curves when a change in phase assemblage occurs.

Figure 11 shows the amount of heat that is removed in the freezing and cooling of one gram-atom of molten copper-zinc alloy from 1400 K. In the case of alloys for which the experimental measurement of heat content was not made at 1400 K, the heat content for this temperature was determined on the assumption that Kopp's Law applies. The copper-zinc phase diagram was used as a guide in determining phase boundaries. Table II shows the phase assemblages present in different areas at different compositions and temperatures.

The lower part of Fig. 11 (below curve AA) represents the liquid phase, while curve AA itself represents the amount of heat removed in cooling a liquid copper-zinc alloy from 1400 K down to the liquidus temperature. The open circles indicate the experimental data points used in the construction of curve AA. Curve

Table II. Phase Assemblages (Fig. 11)*

(1) alpha	(13) alpha + liquid
(2) alpha + beta	(14) alpha + beta + liquid
(3) beta	(15) beta + liquid
(4) beta + gamma	(16) beta + gamma + liquid
(5) gamma	(17) gamma + liquid
(6) gamma + delta	(18) gamma + delta + liquid
(7) gamma + epsilon	(19) delta + liquid
(8) delta + epsilon	(20) delta + epsilon + liquid
(9) delta + gamma + epsilon	(21) epsilon + liquid
(10) epsilon	(22) epsilon + eta + liquid
(11) epsilon + eta	(23) eta + liquid
(12) eta	(24) liquid

*Numbers refer to region numbers in Fig. 11; the corresponding phase assemblage is listed alongside.

BB, on the other hand, represents the amount of heat removed in cooling and freezing of a molten copper-zinc alloy from 1400 K to the solidus temperature, with the experimental data points being represented by squares.

Isotherms (individual data points represented as triangles) are superimposed on this figure. They were constructed from experimental data points. The isotherms indicate the relation between the amount of heat released in cooling alloys from 1400 K to a specified temperature and alloy composition.

The region between curves AA and BB represents the heat effects during the solidification of molten copper-zinc alloys. Triangular areas on this figure are associated with invariant (three-phase) equilibrium. Thus, regions 14, 16, 18, 20, and 22 represent the peritectic reactions L + $\alpha \rightleftharpoons \beta$ (1175 K), L + $\beta \rightleftharpoons \gamma$ (1107 K), L + $\gamma \rightleftharpoons \delta$ (973 K), L + $\delta \rightleftharpoons \epsilon$ (871 K), and L + $\epsilon \rightleftharpoons \eta$ (697 K). The nontriangular regions be-

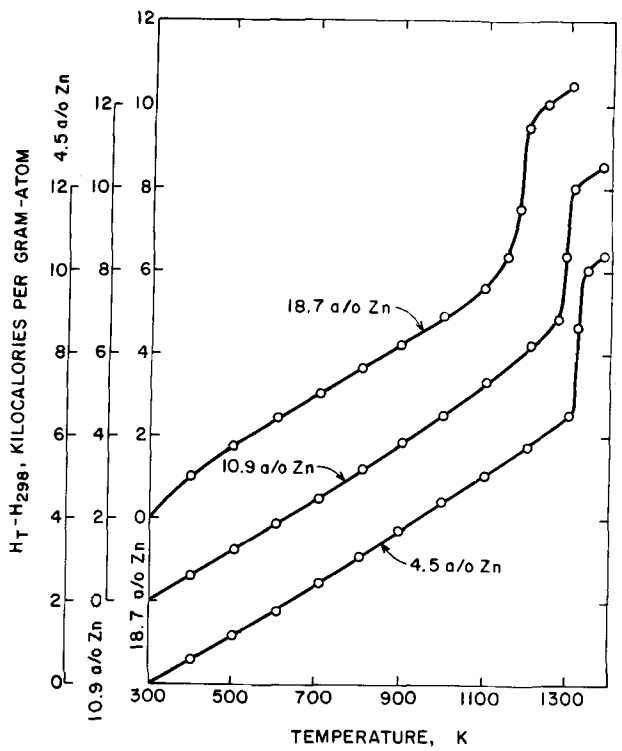

Fig. 6—Enthalpies of Cu-Zn alloys containing 4.5, 10.9, and 18.7 at. pct zinc.

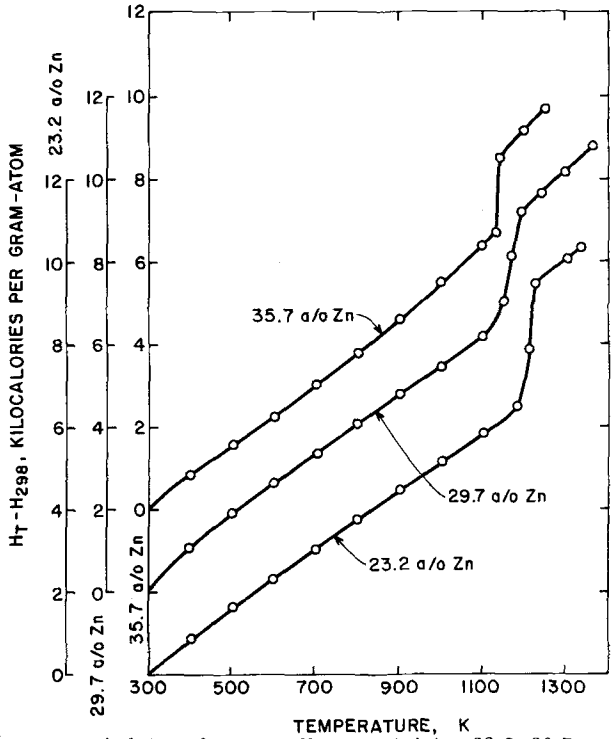

Fig. 7—Enthalpies of Cu-Zn alloys containing 23.2, 29.7, and 35.7 at. pct zinc.

tween curves AA and BB represent the total heat effects of nonisothermal solidification through two phase regions (Regions 13, 15, 17, 19, 21, and 23). This heat effect in alloys that solidify to α solid solution is around 3000 cal/gm-atom. For alloys solidifying to β solid solution, this heat effect is around 2000 cal/gm-atom. For α, δ, and ϵ alloys, it is about 2500 cal/gm-atom and 1750 cal/gm-atom for alloys solidifying to the η phase.

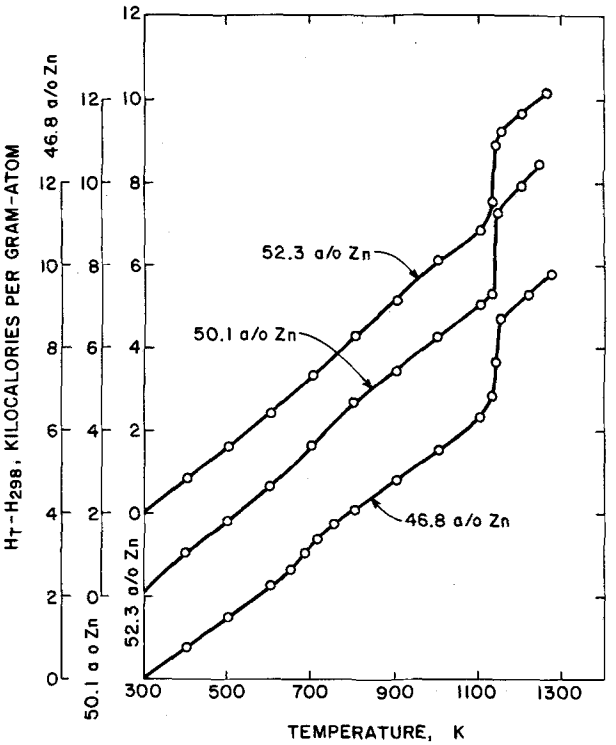

Fig. 8—Enthalpies of Cu-Zn alloys containing 46.8, 50.1, and 52.3 at. pct zinc.

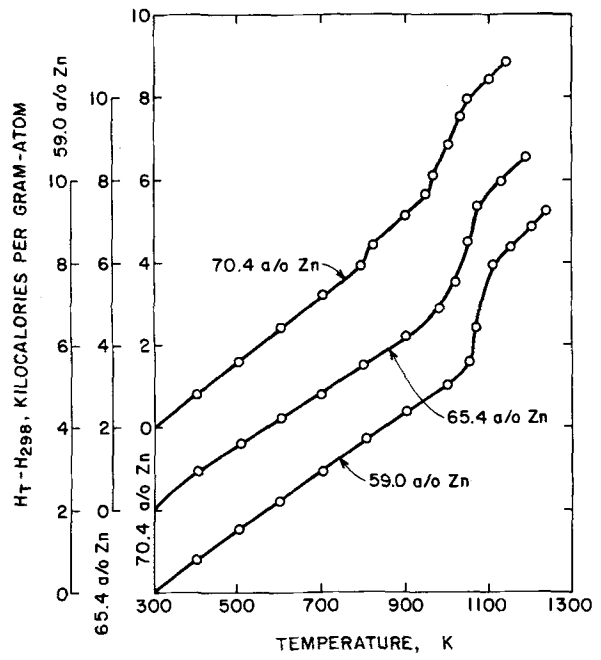

Fig. 9—Enthalpies of Cu-Zn alloys containing 59.0, 65.4, and 70.4 at. pct zinc.

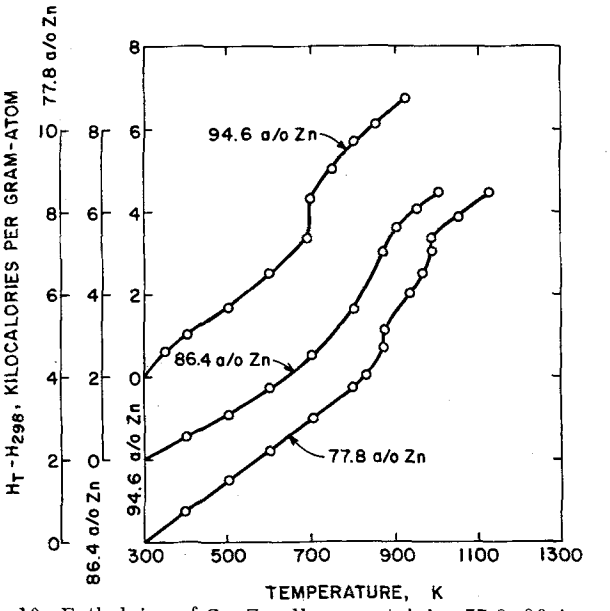

Fig. 10—Enthalpies of Cu-Zn alloys containing 77.8, 86.4, and 94.6 at. pct zinc.

The triangular area designated as Region 9 represents the eutectoid reaction $\delta \rightarrow \alpha + \epsilon$ (831 K).

The heats from the formation of solid copper-zinc alloys at 773 K, after Hultgren *et al*,[2] were combined with enthalpy measurements taken in this investigation to calculate the heats of formation of liquid copper-zinc alloys at 1400 K. These calculated heats of formation of liquid copper-zinc alloys were used to calculate the heats of formation of solid phases at different temperatures. The calculational scheme for the heats of formation of copper-zinc alloys is presented in Appendix II.

As indicated earlier the uncertainty in enthalpy measurements is less than ±180 cal/gm-atom. The uncertainty in the selected values of heats of formation of solid phases at 773 K is ±150 cal/gm-atom up to

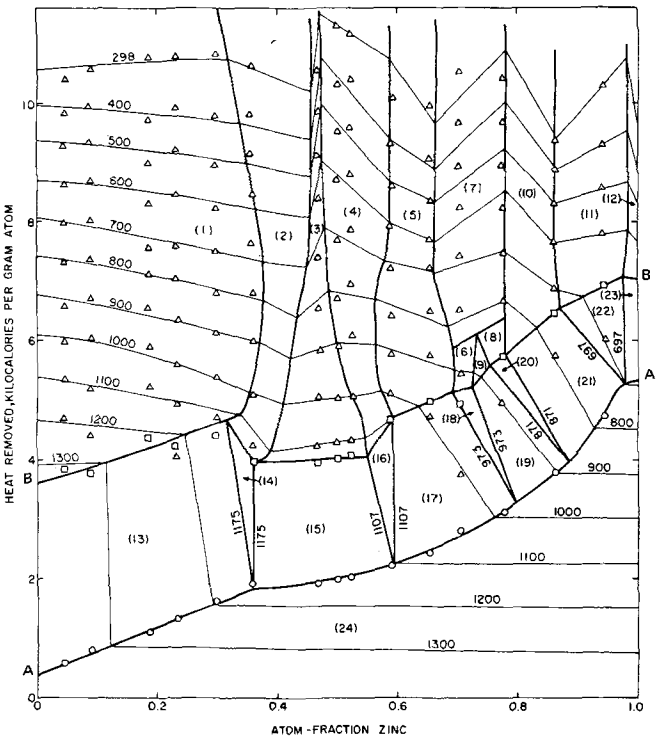

Fig. 11—Heat removed in cooling liquid copper-zinc alloys from 1400 K. (See Table II for phase assemblages corresponding to numbered regions on this figure.)

X_{Zn} = 0.381 where α is stable, and ±300 cal/gm-atom between X_{Zn} = 0.44 and X_{Zn} = 0.488 when β is stable.[2] The heats of formation of liquid copper-zinc alloys are thus accurate to within ±235 cal/gm-atom for compositions up to X_{Zn} = 0.381 and ±350 cal/gm-atom between X_{Zn} = 0.44 and X_{Zn} = 0.488. The uncertainty in the selected values for heats of formation at 773 K in other regions was not reported.

Figure 12 presents the heats of formation of liquid copper-zinc alloys at 1400 K. The curve presented for the heats of formation for 1300 K represents the selected values of Hultgren *et al.*[20] These are accurate to within ±500 cal/gm-atom.

The heats of formation of solid phases are shown in Fig. 13, along with the results of other investigators, and are tabulated in Table III.

The results of Orr and Argent[21] at 573 K for alpha phase alloys agree well with the results of this investigation at 600 K. The heats of formation of alpha phase at 298 K of Kleppa and King[22] agree with this investigation up to 10 at. pct zinc, but are less exothermic for higher zinc alloys. The vapor pressure data of Herbenar *et al*[4] yield heats of formation (calculated by Kubaschewski and Caterall[5]) that are more exothermic than those of Kleppa and King,[22] but less exothermic than obtained from this investigation. Blair and Downie[23] report heats of formation for a 26 at. pct zinc alloy at 673 K of −1390 cal/gm-atom; at 573 K of −1635 cal/gm-atom. By linear extrapolation of these results to 298 K, one obtains a heat of formation at that temperature of −2310 cal/gm-atom, which is fairly good agreement with this investigation. The present results for the heats of formation are reasonably consistent with those of Orr and Argent[21] thus tending to confirm their postulation that a fairly high degree of short-range ordering is developed in alpha phase alloys as the alpha/alpha plus beta phase boundary is approached. Further support for this postulate may be drawn from the fact that the enthalpy-temperature plots for these alloys change slope around 500 K, with an X-ray phase identification showing these alloys to be alpha solid solution.

There is also fairly good agreement between the results of this investigation for the beta, gamma, and

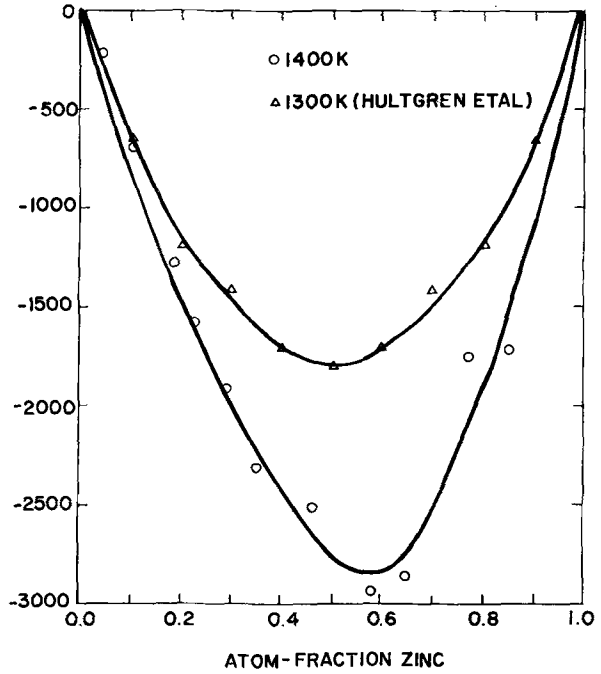

Fig. 12—Heats of formation of liquid Cu-Zn alloys.

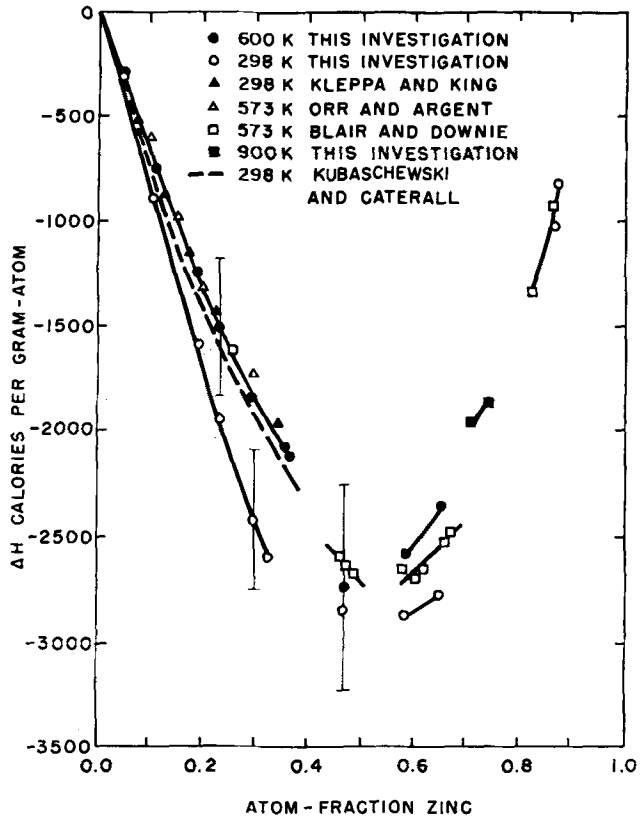

Fig. 13—Heats of formation of solid Cu-Zn alloys.

Table III. Heats of Formation of Solid Copper-Zinc Alloys

Atom-Fraction of Zinc	Phase	$-\Delta H$ of Formation of Alloy at Temperature Indicated, cal/gm-atom				
		298 K	573 K[23] (Ref. 23)	600 K	773 K[2] (Ref. 2)	900 K
0.100	alpha	800		690	630	
0.200	alpha	1690		1340	1310	
0.300	alpha	2490		1870	1750	
0.317	alpha	2640*		–	–	
0.365	alpha	–		2140*		
0.381	alpha	–		–	1970*	
0.440	beta	–		–	2110*	
0.460	beta prime	–	2600	–	–	
0.468	beta prime	2870	–	2870	–	
0.480	beta prime	–	2660	–	–	
0.488	beta	–	–	–	2250*	
0.491	beta prime	–	2680	–	–	
0.582	gamma	–	–	–	2620*	
0.585	gamma	–	2660	–	–	
0.590	gamma	2900*	–	2590	–	
0.600	gamma	3030	2670	2710	2730	
0.654	gamma	2730*	–	2350*	–	
0.664	gamma	–	2540*	–	–	
0.672	gamma	–	–	–	2590*	
0.728	delta	(stable only between 831 K and 973 K)				1970*
0.741	delta	(stable only between 831 K and 973 K)				1870*
0.761	epsilon	–	–	–	2050*	
0.800	epsilon	–	–	–	1840	
0.824	epsilon	–	1440	–	–	
0.847	epsilon	–	–	–	1480*	
0.865	epsilon	830	930	1040	–	

*Refers to phase boundary compositions.

epsilon phases at 600 K and those of Blair and Downie[23] at 573 K. The present investigation yielded slightly more exothermic values for the beta prime phase and slightly less exothermic values for the gamma phase.

For a 46.8 at. pct zinc alloy, a heat effect for the beta-beta prime transformation was estimated as 425 cal/gm-atom. This was obtained by extrapolating the nearly straight line portions above and below the inflection (Fig. 7) and measuring the distance between them at the midpoint. This value agrees well with the value of 450 cal/gm-atom derived from enthalpy data on beta and beta prime phases selected by Hultgren *et al*[2] for a 47.5 at. pct zinc alloy.

The excess entropies of formation of alpha phase alloys are presented in Fig. 14 as a function of the zinc content of the alloys. The excess free energies from the work of Argent and Wakeman[8] were combined with the heats of formation to yield excess entropies. Almost ideal entropy is exhibited up to 9 at. pct zinc. The negative values of excess entropies can be explained if short-range order persists to comparatively high temperatures in alpha phase alloys containing more than 9 at. pct zinc, and the degree of ordering increases as the alpha/alpha plus beta boundary is approached. Table IV presents the excess entropies for beta prime, gamma, and epsilon phases. These were calculated from the free-energy data of Hultgren *et al*[20] and the heats of formation from this investigation.

The value of the excess entropy of formation of -1.15 e.u. for the beta prime phase is slightly higher than the value of -1.3 reported by Hultgren *et al*,[20] but lower than the value of -0.93 reported by Blair and Downie.[23] For the gamma phase the values are lower

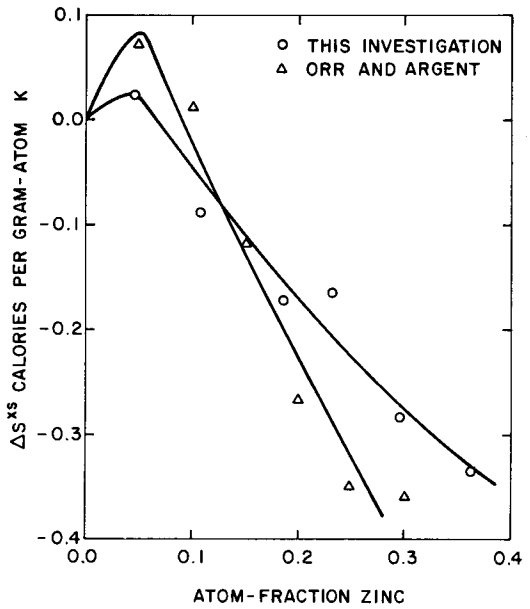

Fig. 14—Excess entropies of formation of alpha phase Cu-Zn alloy at 1000 K.

than those reported by Blair and Downie[23] of -0.52 e.u., but higher than the value of -1.0 estimated by Hultgren *et al*.[20] For the epsilon phase, a value of 0.2 e.u. was obtained that agrees with a value of 0.15 obtained by Blair and Downie[23] for a 0.82 at. pct zinc alloy, Hultgren *et al*[20] estimate a value of -0.2 e.u.

The rather low values of excess entropies for the beta prime and gamma phases are probably related to the fact that there is short-range order in these phases. In contrast, the epsilon phase and alpha phase at lower zinc contents show small excess entropies; at higher zinc contents the value of the excess entropy for alpha phase alloys becomes more negative, indicating a tendency towards ordering.

SUMMARY

When the diversity of experimental techniques used by various investigators in determining thermodynamic data is taken into account, the agreement of the heats of formation determined in the present study with prior ones in general seems satisfactory.

This method of continuous calorimetry appears to be capable of measuring high-temperature enthalpies within 95 pct confidence limits of ±180 cal/gm-atom, or 2.5 pct of the heat measured. Therefore, it may be suitable for obtaining data useful in engineering applications of systems for which heats of formation data are unavailable.

Table IV. Excess Entropies of Formation of Beta Prime, Gamma, and Epsilon Phases

Temperature, K	At. Pct Zinc	Phase	Excess Entropy, e.u.
623	46.8	Beta Prime	–1.15
733	59.0	Gamma	–0.78
	65.4	Gamma	–0.90
733	86.4	Epsilon	0.20

Appendix I. Conversion to SI Units

Quantity	Unit Used in the Text	SI-Based Unit	Conversion Factor
Heat (energy)	calorie	Joule	1 cal = 4.1868 Joule
	kilocalorie	Joule	1 kilocalorie = 4186.8 Joule
Enthalpies Heat contents, Heats of formation	kilocalorie per gram-atom	Joule per kilogram-atom	1 kilocalorie per gram-atom = 4.1868×10^6 Joule per kilogram-atom
Entropy	kilocalorie per gram-atom K	Joule per kilogram-atom K	1 kilocalorie per gram-atom K = 4.1868×10^6 Joule per kilogram-atom K

Appendix II. Heat of Formation of Liquid Solution at 1400 K

$$\text{Liq Soln}(X_{Zn}, 1400) = X\,\text{Zn(L, 1400)} + (1-X)\text{Cu (L, 1400)} \quad -\Delta H_{LS}$$
$$X\,\text{Zn(L, 1400)} = X\,\text{Zn(L, 773)} \quad - X(H_{1400,L} - H_{773,L})_{Zn}$$
$$X\,\text{Zn(L, 773)} = X\,\text{Zn('S', 773)} \quad - X(\Delta H_f)_{Zn}$$
$$(1-X)\text{Cu(L, 1400)} = (1-X)\text{Cu(S, T)} \quad -(1-X)(H_{1400,L} - H_{773,S})_{Cu}$$
$$X\,\text{Zn('S', 773)} + (1-X)\text{Cu(S, 773)} = \text{Sol Soln}(X_{Zn}, 773) \quad + \Delta H_{SS,773}$$

$$\text{Liq Soln}(X_{Zn}, 1400) = \text{Sol Soln}(X_{Zn,773}) \quad + \Delta H_{exp}$$
$$\Delta H_{LS} = -\Delta H_{exp} - X(H_{1400,L} - H_{773,L} + \Delta H_f)_{Zn} - (1-X)(H_{1400,L} - H_{773,S})_{Cu} + \Delta H_{SS,773}$$

Specimen Calculation:

$X_{Zn} = 0.187$

$H_{Zn} = (H_{1400,L} - H_{773,L} + \Delta H_f)_{Zn} = 6468$ cal (Hultgren[24])

$H_{Cu} = (H_{1400,L} - H_{773,S})\text{Cu} = 7586$ cal (Hultgren[2])

$\Delta H_{exp} = -7260$ cal

$\Delta H_{SS,773} = -1220$ cal (Hultgren[2])

$XH_{Zn} = 1210(1-X)H_{Cu} = 6167$

$\Delta H_{LS} = 7260 - 1210 - 6167 - 1220 = -1337$ cal.

Heat of Formation of Solid Solution at T, K

$$\text{Liq Soln}(X_{Zn}, 1400) = X\,\text{Zn(L, 1400)} + (1-X)\text{Cu(L, 1400)} \quad -\Delta H_{LS}$$
$$X\,\text{Zn(L, 1400)} = X\,\text{Zn(L, T)} \quad - X(H_{1400,L} - H_{T,L})_{Zn}$$
$$X\,\text{Zn(L, T)} = X\,\text{Zn('S', T)} \quad - X(\Delta H_f)\text{Zn}$$
$$(1-X)\text{Cu(L, 1400)} = (1-X)\text{Cu(S, T)} \quad -(1-X)(H_{1400,L} - H_{T,S})_{Cu}$$
$$X\,\text{Zn(S, T)} + (1-X)\text{Cu(S, T)} = \text{Sol Soln}(X_{Zn}, T) \quad + \Delta H_{SS}$$

$$\text{Liq Soln}(X_{Zn}, 1400) = \text{Sol Soln}(X_{Zn}, T) \quad + \Delta H_{exp}$$
$$\Delta H_{SS} = \Delta H_{exp} + \Delta H_{LS} + X(H_{1400,L} - H_{T,L} + \Delta H_f)_{Zn} + (1-X)(H_{1400,L} - H_{T,S})_{Cu}$$

Specimen Calculation:

$T = 600$ K Phase Alpha

$X_{Zn} = 0.187$

$H_{Zn} = 7700$ cal (Hultgren[24]) $H_{Cu} = 8693$ cal (Hultgren[2])

$XH_{Zn} = 1440$ cal $(1-X)H_{Cu} = 7067$

$\Delta H_{LS} = -1270$

$\Delta H_{exp} = -8500$

$\Delta H_{SS} = -8500 - 1270 + 1440 + 7067 = -1263$ cal.

ACKNOWLEDGMENTS

This work was made possible by the generous support received from the International Copper Research Association.

REFERENCES

1. J. Lumsden: *Thermodynamics of Alloys,* pp. 256-74, Institute of Metals, London, 1952.
2. R. Hultgren and P. D. Desai: *INCRA Series on the Metallurgy of Copper, I.,* pp. ii, 18-28, 182-95, 1971.
3. R. Hargreaves: *J. Inst. Metals,* 1939, vol. 64, pp. 115-34.
4. A. W. Herbenar, C. A. Siebert, and O. S. Duffendack: *Trans. AIME,* 1950, vol. 188, pp. 323-26.
5. O. Kubaschewski and J. A. Caterall: *Thermochemical Data of Alloys,* pp. 66-69, Pergamon Press, London and New York, 1956.
6. J. P. Pemsler and E. J. Rapperport: *Trans. TMS-AIME,* 1969, vol. 245, pp. 1395-1400.
7. E. J. Rapperport and J. P. Pemsler: *Met. Trans.,* 1972, vol. 3, pp. 827-31.
8. B. B. Argent and D. W. Wakeman: *Trans. Faraday Soc.,* 1958, vol. 54, pp. 799-806.
9. A. Olander: *Z. Phys. Chem.,* 1933, vol. 164, pp. 428-38.
10. O. J. Kleppa and C. E. Thalmayer: *J. Phys. Chem.,* 1959, vol. 63, pp. 1953-58.
11. D. B. Downie: *Acta Met.,* 1964, vol. 12, pp. 875-82.
12. L. H. Everett, P. W. M. Jacobs and J. A. Kitchner: *Acta Met.,* 1957, vol. 5, pp. 281-84.
13. L. H. Baker: *Trans. Inst. Min. Met.,* Section C: Mineral Processing and Extractive Metallurgy, 1970, vol. 79, pp. C1-C5.
14. W. Oelsen, E. Schürmann, and G. Heynert: *Arch. Eisenhuettw.,* 1955, vol. 26, pp. 19-24.
15. W. Oelsen, K. H. Rieskamp, and O. Oelsen: *Arch. Eisenhuettw.,* 1955, vol. 26, pp. 253-66.
16. W. Oelsen, E. Schürmann, and C. Florin: *Ibid.,* 1961, vol. 32, pp. 719-28.
17. K. Yamaguchi and G. W. Healy: *Met. Trans.,* 1974, vol. 5, pp. 2591-96.
18. K. Yamaguchi and G. W. Healy: *Trans. TMS-AIME,* 1966, vol. 236, pp. 944-46.
19. K. K. Kelley: U. S. D. I. Bureau of Mines Bull., p. 584, 1960.
20. R. Hultgren, R. L. Orr, P. D. Anderson, and K. K. Kelley: *Selected Values of Thermodynamic Properties of Metals and Alloys,* pp. 712-23, John Wiley, New York and London, 1963.
21. R. L. Orr and B. B. Argent: *Trans. Faraday Soc.,* 1965, vol. 61, pp. 2126-31.
22. O. J. Kleppa and R. C. King: *Acta Met.,* 1962, vol. 10, pp. 1183-86.
23. G. Blair and D. B. Downie: *J. Metal Sci.,* 1970, vol. 4, pp. 1-5.
24. R. Hultgren, P. D. Desai, D. T. Hawkins, M. Gleiser, K. K. Kelley, and D. T. Wagman: *Selected Values of Thermodyamic Properties of the Elements,* pp. 565-74, American Society for Metals, Ohio, 1973.